Damage Characteristics of RC Bridge Columns with Interlocking Spirals under Combined Cyclic Loading Including Torsion

Qian Li & Abdeldjelil Belarbi
Department of Civil and Environmental Engineering, University of Houston, USA

SUMMARY:
This paper presents the test results of three RC bridge columns with double interlocking spirals under cyclic pure torsion and combined action of cyclic flexural and torsional moments. The damage characteristics of these columns under combined loadings are investigated by extending the existing damage indices for flexural failure mode to pure torsion and combined loading from the perspective of performance-based seismic design. According to various damage limit states, the damage index models under pure torsion and decoupled damage index models for torsion and bending-shear, respectively, under combined loading are developed to evaluate the damage states in terms of progression of damage. Also, the dissipated flexural and torsional energy of three columns for each individual loading cycle and the accumulated dissipated energy with respect to different failure modes are discussed and highlighted, which is an important parameter in assessing the strength and stiffness degradation of reinforced concrete members subjected to cyclic loading.

Keywords: RC bridge columns; interlocking spirals, combined loadings; damage index; torsion

1. GENERAL INSTRUCTIONS

Reinforced concrete (RC) bridge columns can be designed to specific damage levels for different earthquake motions by using the performance-based design approach. In the process of performance-based design, the analytical damage index models are necessary to define the damage states and quantify the damage in terms of strain and ductility levels. Performance of the RC bridge columns under different levels of earthquake can be evaluated from the predicted hysteresis curves using the damage indices. Hence, a proper damage index model numerically quantifying the damage states should be developed including the essential parameters that describe the hysteretic behavior under combined loadings during earthquakes. A few studies (Zahrah and Hall 1984, Hwang, T.H. 1984, Park, Y.J. 1985, Williams, M.S. 1997, Hindi, R.A. 2001, Khashaee, 2005) were conducted to investigate the development of damage indices based on flexural behavior. However, RC bridge columns could be subjected to a combination of flexural, axial, shearing, and torsional loads during earthquake excitations. The combination of seismic loadings can result in complex flexural and shear failure of bridge columns due to irregular structural configurations, especially in skewed or horizontally curved bridges, bridges with unequal spans or column heights, and bridges with outrigger bents, arch ribs and L shaped bridge piers. The location and distribution of the plastic hinge vary along the height of columns due to the addition of torsional loading. In addition, the flexural and torsional strength and stiffness degrade more rapidly under the combined loading. According to literature review, there have been few experimental studies on development of damage indices to predict the progression of damage under combined loadings including torsion (Suriya and Belarbi, 2008). In order to establish the performance-based design approach for RC bridge columns under combined loadings, three oval RC columns with interlocking spirals were tested under combined loading with various torsional-and-bending moment ratios of 0.2, 0.6 and ∞ respectively. Accordingly a damage index model for pure torsion and decoupled damage index models for combined loading are developed in this paper.

2. PREVIOUS RESEARCH AND PROPOSED DAMAGE INDEX

In the process of the performance-based design approach, the non-dimensional parameter known as "damage index" can be used to perform a quantitative assessment of various damage states under earthquake excitations. In the earlier study, noncumulative damage indices can be simply measured based on displacement ductility or inter-storey drift, which do not consider the strength or stiffness degradation and energy dissipation under cyclic loadings. Later on, the damage was indicated by the degradation of stiffness proposed by Banon et al., which is defined as the ratio of initial stiffness to the secant stiffness corresponding to the maximum displacement in a given loading cycle. Recently, the formula of this indicator has been modified by Roufaiel and Meyer in terms of stiffness or flexibility. However, the damage to a structure or its components is caused by the cyclic loading or deformation during an earthquake. The RC members suffered both strength and stiffness degradation under cyclic loading and the local damage characteristics in these members are cumulative in nature during various damage limit states. Therefore, the cumulative damage indices based on ductility, displacement, or energy dissipation were developed to account for all these cumulative and deteriorative natures. In order to reflect the cumulative damage characteristics, Banon et al. (1981) proposed an approach to measure the cumulative ductility for all the loading cycles, which included both the elastic and plastic response under cyclic loads. Zahrah and Hall (1984) proposed to use the numbers of equivalent yield excursions to assess the damage in structures, based on the maximum hysteretic energy demand, displacement ductility, and yield strength of the members. Hwang and Scribner (1984) adopted stiffness and energy dissipation along with displacement in a given loading cycle to represent cumulative damage characteristics of members under cyclic loading, whose main disadvantage is the difficulty to quantify the damage limit states and its maximum value is not unity. Park and Ang (1985) linearly combined the ductility ratio as the primary variable and the normalized cumulative energy as the secondary item to quantify the flexural damage under cyclic loading. Williams, M.S. (1997) conducted a series of single-component tests using a variety of moment to shear ratios and stirrup spacing to compare and evaluate the existing eight damage indices. On the basis of these comparisons, it concluded that the more sophisticated indices gave no more reliable an indication of damage than simple measures such as ductility and stiffness degradation. Hindi, R.A. (2001) proposed and verified a damage model combining ductility, energy, and low cycle fatigue damage, which provided a realistic prediction of damage throughout the loading cycles for flexure and shear dominated test columns. Khashaee, P. A (2005) summarized existing damage index models and proposed a new damage index associated with ductility and stiffness degradation which has a strong correlation with the portion of the earthquake energy associating with inelastic action. However, these damage index models are limited in cyclic flexure and shear dominated failure modes.

Torsional damage index model and decoupled flexural and torsional damage index models for combined loading including torsion must be developed to identify the implications of combined loading from the perspective of performance-based seismic design. The non-linear flexural and torsional hysteretic response of a column subjected to a combined cyclic loading and the damage indices of them were obtained directly from the experimental study to validate that the decoupled flexural and torsional damage indices can be classified to represent the various damage limit state of RC columns. The Park and Ang damage index and the normalization-modified Hwang and Scribner damage index are used to quantify the flexural damage under combined loading. Based on these two approaches, torsional damage index models are developed for the RC columns under pure torsion and combined loading including torsion. So the flexural and torsional damage indices can be decoupled to distinguish the effect of flexural and torsional behavior from the combined loading condition. The verification of the proposed damage index model is discussed in following sections.

2.1. Flexural Damage Index for Combined Loading

The Park and Ang (1985) model is the most widely used damage index, which can be used for RC columns to quantify the flexural damage under combined loading as following given by Eq. (2.1):

$$FDI_{\text{Flexure,Combined Loading}} = \frac{u_m}{u_u} + \beta \frac{E_{hm}}{Q_y u_u} \tag{2.1}$$

Where, u_m is maximum displacement achieved in the loading cycle m; $u_u$is ultimate displacement under monotonic load; u_y is yield rotation; β is constant accounting for the effect of cyclic load taken as 0.05; E_{hm} is maximum hysteretic energy demand; and Q_y is yield strength of the structure or member. The main advantage of Park and Ang damage index model is its simplicity and physical intuition as it varies from '0' responding to no damage to '1' responding near collapse. The damage index model proposed by Hwang and Scribner was modified by normalization with respect to totally cumulative flexural energy dissipated under flexure ($E_{Total,Flexure}$) to predict the flexural damage index under combined loading as shown in Eq. (2.2):

$$FDI_{Flexure,Combined\ Loading} = \frac{\sum_{i=1}^{M} \Delta E_{h,i} \frac{K_{m,i} u_{m,i}^2}{K_0 \quad u_y^2}}{E_{Total,Flexure}} \tag{2.2}$$

Where, i is the cycle number, M is the total number of yield cycles, K_0 is the pre-yield flexural stiffness, $u_{m,i}$ is the maximum displacement in the i^{th} loading cycle, K_{mi} is the secant flexural stiffness corresponding to $u_{m,i}$, $\Delta E_{h,i}$ is the hysteretic dissipated energy in the i^{th} load cycle, and u_y is the yielding displacement.

2.2. Torsional Damage Index for Combined Loading

In this study, the cumulative damage index model proposed by Park and Ang (1985) was modified to predict the progression of torsional damage state under pure torsion and combined loading. The following Eq. (2.3) is thus proposed for torsional damage indices respectively under pure torsion and combined loadings:

$$TDI_{Torsion,Combined\ Loading} = \frac{\theta_m}{\theta_u} + \beta \frac{E_{hm}}{T_y \theta_u} \tag{2.3}$$

Where, θ_m is maximum rotation achieved in the loading cycle m; $\theta_u$is ultimate rotation under monotonic load; θ_y is yield rotation; β is constant accounting for the effect of cyclic load taken as 0.05; E_{hm} is maximum hysteretic energy demand; and T_y is yield strength of the structure or members. The normalization-modified Hwang and Scribner model from totally cumulative flexural energy ($E_{Total,Torsion}$) was also used to quantify the various torsional damage states as shown in Eq. (2.4):

$$TDI_{Torsion,Combined\ Loading} = \frac{\sum_{i=1}^{M} \Delta E_{h,i,T} \frac{K_{m,i,T} \theta_{m,i,T}^2}{K_{0,T} \quad \theta_{y,T}^2}}{E_{Total,Torsion}} \tag{2.4}$$

Where, i is the cycle number, M is the total number of yield cycles, $K_{0,T}$ is the pre-yield torsional stiffness, $\theta_{m,i,T}$ is the maximum rotation in the i^{th} loading cycle, $K_{m,i,T}$ is the secant torsional stiffness corresponding to $\theta_{m,i,T}$, $\Delta E_{h,i}$ is the hysteretic dissipated energy in the i^{th} load cycle, and $\theta_{y,T}$ is the yielding displacement.

3. EXPERIMENTAL PROGRAM AND RESULTS DISCUSSION

Specimen and Test Setup: In order to validate the proposed damage index models, three half-scale oval RC columns with interlocking spirals were designed to represent typical existing bridge columns as shown in Fig. 1Error! Reference source not found.. Each of the columns was fabricated with the oval cross section of 610 mm×915 mm and the clear concrete cover of 25 mm. The total height of columns was 4.2 m with an effective height of 3.35 m measured from the top of footing to the centerline of applied loads. The columns were tested under combined loading at T/M ratios of 0.2, 0.6, and ∞. Twenty No. 8 bars (25 mm in diameter) was used to provide a longitudinal reinforcement ratio of 2.13%. Spiral

reinforcement was provided by No. 4 bars (12.5 mm in diameter) with a pitch of 70 mm to obtain transverse reinforcement ratios of 1.32%. An axial load, which is equivalent to 7% of the axial capacity of columns, was applied before applying flexure and torsion to simulate the superstructure dead load on the column in a bridge system. The average concrete compressive strength of all columns was about 36 MPa on the day of testing; and the average yield strength of reinforcement was about 490 MPa. Cyclic torsion and combined cyclic flexure, shear and torsion were applied by controlling the imposed force or displacement of two horizontal servo-controlled hydraulic actuators as shown in Fig. 2. Cyclic pure torsion was created by imposing equal but opposite directional forces with the two actuators. Combined cyclic torsional and flexural moments were generated by applying different specific forces or displacements with each actuator. The ratio of the imposed flexural moment to torsional moment was controlled by maintaining the specific forces or displacements in the two actuators. A hydraulic jack was placed on top of the columns to apply for axial load measured by a load cell between the hydraulic jack and the top of the load stub. The twist and horizontal displacements of the columns were measured by string transducers at multiple heights above the column footing. Electrical strain gages were attached to the surface of the spirals and longitudinal reinforcement then mounted at various heights along the whole column based on T/M ratios.

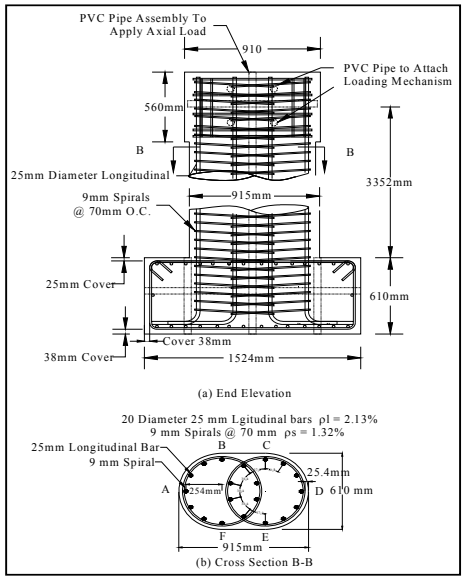

Figure 1. Sectional Details of Oval Column with Interlocking Spirals.

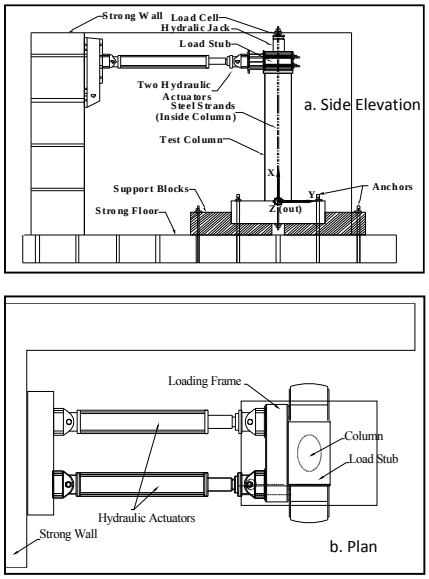

Figure 2. Test Setup

Loading Protocol: Testing of the columns under combined flexure, shear, and torsion were conducted in load control mode up to the first yielding of the longitudinal bars (F_y). The horizontal displacement corresponding to F_y was defined as a displacement ductility one ($\mu_\Delta=1$). The column under pure torsion was loaded in load control mode up to the first yielding of transverse bar (T_y). The rotation corresponding to T_y was defined as a twist ductility one ($\mu\theta=1$). After the first yield, the tests were conducted in displacement control mode until the ultimate failure of the columns. Meanwhile, T/M ratios were controlled at the designed value of 0.2, 0.6, and ∞. Three cycles of loading mode were performed at each ductility level intending to provide an indication of stiffness degradation characteristics. For flexural moment, the loading in the BF or CE direction was defined as positive and that in the FB or EC direction as negative cycles as shown in Figure 1 (b). For torsional moment, counter-clockwise torque was defined as positive cycles, and the clockwise direction as negative cycles.

Hysteresis Curve and Damage Procession under Cyclic Pure Torsion: The torsional hysteresis curve of the column under pure torsion is shown in Fig. 3. The torsional moment-twist curves

are approximately linear before cracking torsional moment (50% Ty); thereafter they become nonlinear due to concrete cracking and torsional stiffness degradation. During the positive cycles of loading, the two interlocking spirals were unlocked resulting in reduction of the confinement effect on the core concrete and more significant concrete cover spalling. However, during the negative cycles of loading, the two spirals were locked with each other to enhance the confinement of spirals to the core concrete. Hence torsional resistance during the negative cycles was higher than positive cycles at higher ductility levels due to the extra confinement effect caused by the locking and unlocking actions of interlocking spirals. The locking and unlocking effects are shown in the asymmetric nature of the torsional hysteresis curve in Fig. 3. The progression of damage in the column under pure cyclic torsion was indicated in Fig. 4. Significant diagonal cracks started developing near mid-height of the column at post-cracking stage. As the test progressed, diagonal cracks continued to develop at around 45˚ inclination along the format of spirals. The cracks lengthened and widened with the increase of applied torsion before the yield loading as shown in Fig. 4 (a). Concrete cover spalling was observed at ductility level one and the spalling region extended along the whole height of the column when the torsional ductility reached six as shown in Fig. 4 (b). Although the cover concrete spalled along the entire length of the column, significant core concrete crushing led to the torsional plastic hinge near higher mid-height of the column as shown in Fig. 4 (c) which is significantly different from a typical flexural plastic hinge zone located at the bottom of columns. The failure modes were in the sequence of shear cracking, spalling, spiral yielding, longitudinal bar yielding, and then overall failure by significant core concrete degradation and the longitudinal bar twisted extremely. In addition, the longitudinal bars located within the interlocking region transferred the shear stress from spiral to spiral by dowel action of those longitudinal bars considerably contributing to resisting torsional load at high ductility level.

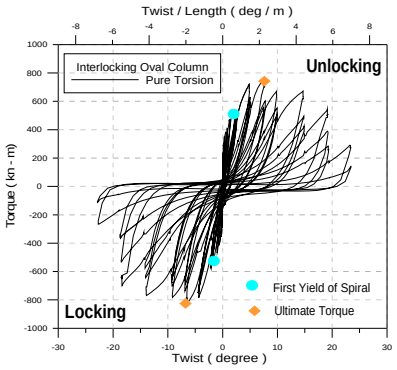

Figure 3. Torsional Hysteresis under Pure Torsion

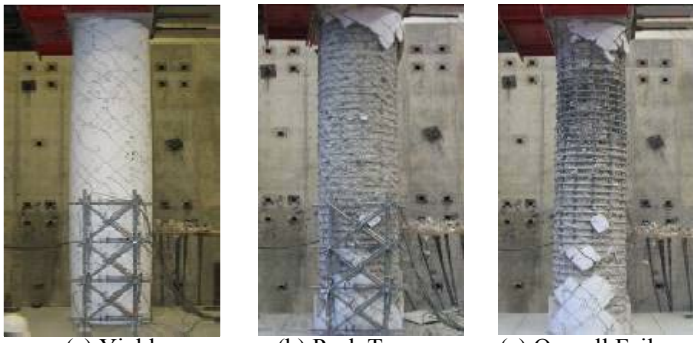

(a) Yield (b) Peak Torque (c) Overall Failure

Figure 4. Damage Progression of Column under Pure Torsion

Hysteresis Curve and Damage Procession under Cyclic Combined Loading: Two columns were tested under combined loading at T/M ratio of 0.2 and 0.6, respectively. The comparison of flexural and torsional hysteresis behaviors were shown in Fig. 5. The flexural cracks were first observed at the interlocking region near the bottom of the column. Then flexural cracks became more inclined and more shear cracks occurred with increasing torsional loading effects. For the column loaded at T/M ratio of 0.6, longitudinal bars and spirals yielded simultaneously at the yield loading F_y which determined the balanced T/M ratio. More intense asymmetric nature of the torsional hysteresis curve was observed in Fig.5 (b) for columns under combined loading as compared to pure torsion. This is because that combined flexure, shear, and torsion resulted in additive shear stress on one side of the cross section during the unlocking cycle leading to more damage and less resistance. Strength and stiffness

degradation were observed with increases in the loading cycles at each ductility level. The flexural and torsional strength reduced considerably due to the effect of combined loading compared to the column under pure flexure and pure torsion. Fig. 6 shows the damage progression of the column under combined loading at T/M ratio of 0.6, which is torsion dominant failure mode as similar to pure torsion. Soon after the yield of longitudinal bar and spirals, concrete cover spalling and large shear crack at an inclination of 45˚ was observed at the middle height of the column as shown in Fig. 6 (1)-(i). The concrete cover spalling region developed downward along the column at the higher ductility level and spread to 2/3 height of the column at final failure stage as shown in Figure 6 (1)-(iii). For the column loaded at T/M ratio of 0.2, longitudinal bar yielded first at the yield loading and spirals yielded later at the higher ductility of six due to the lower T/M ratio. The concrete cover spalling did not happen until higher ductility level three at the bottom of the column, and developed upward along the column to 610 mm height at the final failure. Fig. 6 (2) shows the typical damage progression of the column under combined loading at T/M ratio of 0.2, which is more likely the flexure dominant failure mode. In both columns, failure was initiated by the severe combination of shear and flexural cracks, progressive spalling of the cover concrete; and finally with severe core degradation followed by buckling and breaking of the longitudinal bars. Core degradation locations for these two columns were observed lower than that under pure torsion which indicates the change of the torsional plastic hinge location due to the effect of bending. However, the specific location of the plastic hinge depends on applied T/M ratios.

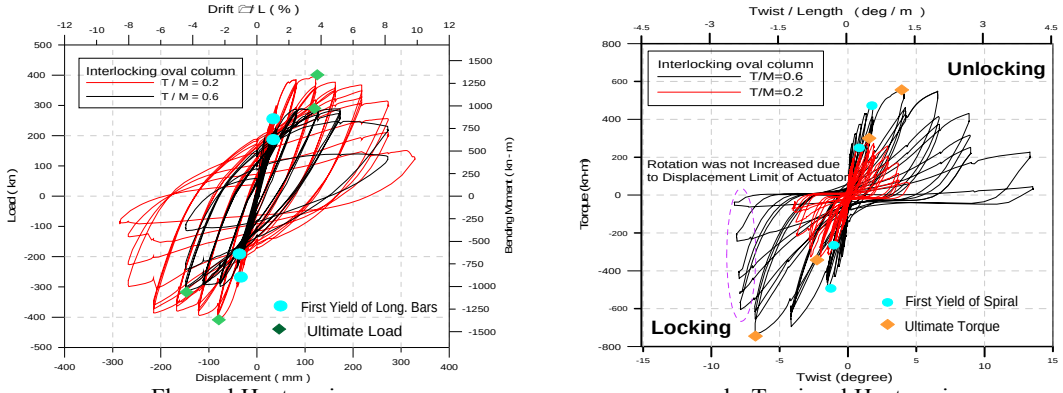

a. Flexural Hysteresis b. Torsional Hysteresis

Figure 5. Comparison of Hysteretic Behavior under Combined Loading

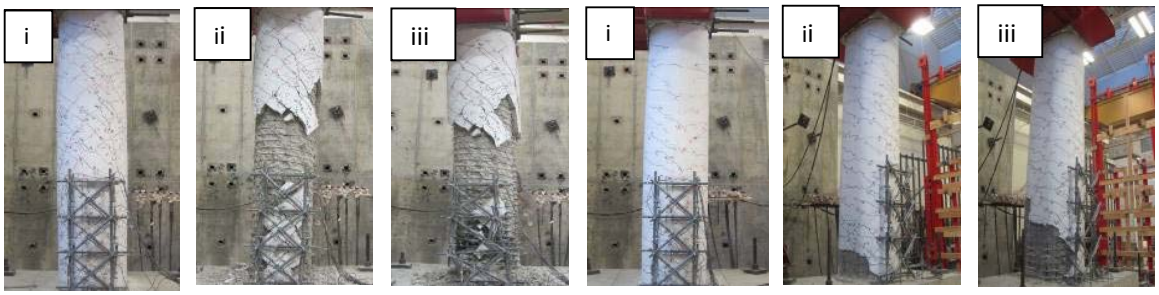

(1) T/M = 0.6 (2) T/M=0.2

Figure 6. Comparison of Damages under Combined Loading at (i) Longitudinal Reinforcement Yield (ii) Peak Load and (iii) Overall Failure

Energy Dissipation: Energy dissipation is an important parameter in assessing the strength and stiffness degradation of reinforced concrete members subjected to cyclic loading of a structure, which are substantially affected by the reinforcement ratio, reinforcement arrangement, plastic deformation,

and axial compressive force. The dissipated flexural and torsional energy in the tested columns are defined as the area enclosed by the load-displacement and torque-rotation hysteresis curve, respectively. The dissipated flexural and torsional energy of three columns for each individual loading cycle and the accumulative dissipated energy are discussed in the following section. The flexural energy dissipation capacity mainly relies on the strength of the concrete and the longitudinal reinforcement, inelastic deformation of reinforcement in the plastic hinge, and the arrangement of longitudinal reinforcement; the torsional energy dissipation capacity is mostly affected by concrete cover, the strength of concrete and transverse reinforcement, and configuration of transverse reinforcement. For the column tested under T/M ratios of 0.2, the dissipated flexural and torsional energy at each cycle was maintained at a low level before the reinforcement yielding due to elastic response of the columns as shown in Figs. 7 and 8. Thereafter, the energy dissipated at the first cycle of the each ductility significantly increased along with the increasing ductility level up to ultimate flexure dominated failure. For the column tested under T/M ratio of 0.6, the dissipated flexural energy developed as the same trend as the one with T/M ratio of 0.2 as shown in Fig. 9; while the dissipated torsional energy at the first cycle of each ductility increased along with the increasing ductility up to peak torque and then decreased for the following imposed ductility as shown in Fig. 10, which resulted from the dominated torsional failure mode and the fact that torsional stiffness severely degraded after the concrete cover totally palled and the peak torque was achieved.

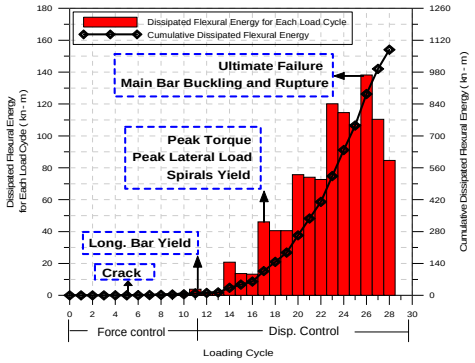

Figure 7. Dissipated Flexural Energy at T/M=0.2

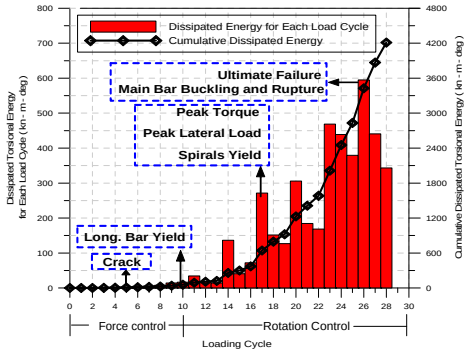

Figure 8. Dissipated Torsional Energy at T/M=0.2

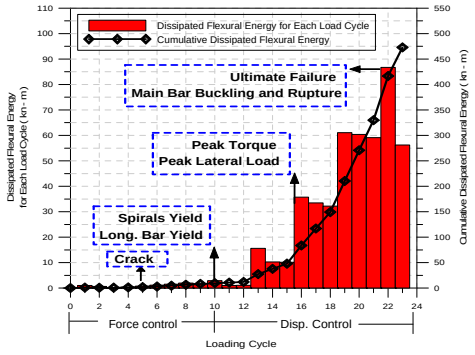

Figure 9. Dissipated Flexural Energy at T/M=0.6

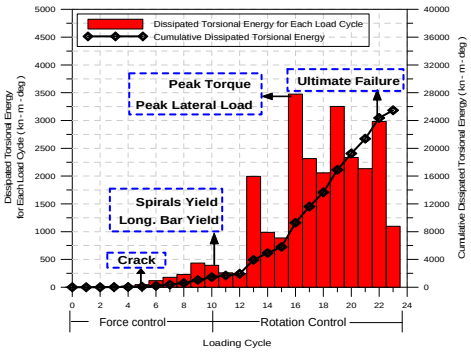

Figure 10. Dissipated Torsional Energy at T/M=0.6

For the column under pure torsion with tensional dominant failure mode, the dissipated torsional energy at the first cycle of each ductility increased up to the peak torque state with total concrete spalling and then continued, increasing until the higher ductility with more crushing of core concrete and twist buckling of longitudinal reinforcement, and finally dropped down at the ultimate failure as shown in Fig. 11. This fact indicated that torsional energy dissipation can be developed more after peak torque state with the contribution from transverse confinement of spirals and dowel action of longitudinal bars. However, the dissipated flexural and torsional energy for all the columns decreased with more loading cycle at each ductility level resulting from the degradation of stiffness. The

comparison of cumulative dissipated flexural and torsional energy for columns with various T/M ratios was summarized in Figs. 12 and 13. Accordingly the dissipated flexural energy decreased significantly as the T/M ratio increases due to the fact that torsion effect causes less displacement ductility capacity, a more severe shear crack, and more stiffness degradation; also, the dissipated torsional energy decreases as the T/M ratio decreases due to the flexure effect such that flexural crack, buckling of longitudinal bar and core concrete crushing. For all three columns, the energy dissipation rate verses deformation ductility increased with an increase in T/M ratio, which indicates that torsional moment in the column under combined loading accelerated the energy dissipation due to the more significant stiffness degradation.

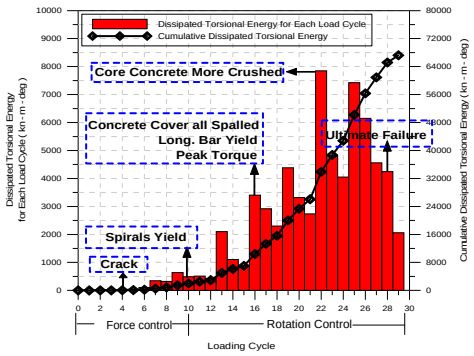

Figure 11. Dissipated Torsional Energy at T/M=∞

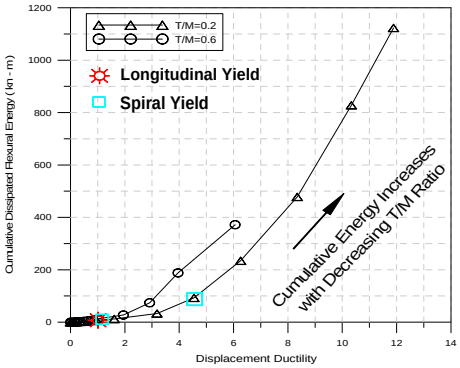

Figure 12. Comparison of Cumulative Flexural Energy Dissipation

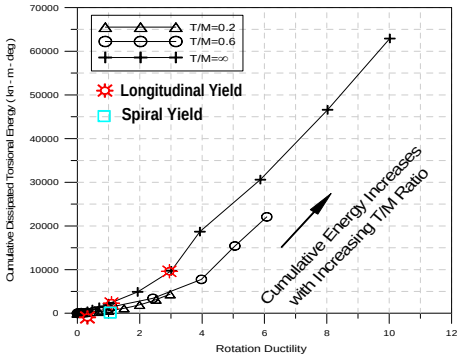

Figure 13. Comparison of Cumulative Torsional Energy Dissipation

4. VALIDATION OF PROPOSED DAMAGE INDEX AND EFFECT OF TORSION

According to the two proposed damage index models stated above, the flexural and torsional damage indexes were calculated from flexural and torsional hysteresis of columns under pure torsion and combined loadings; and the effect of torsion is investigated with respect to various in T/M ratios. The Park and Ang damage index model can well be used to represent the progression of damage limit states for both flexural and torsional hysteresis as shown in Figs. 14 and 15. In both cases, the progression of damage index by the Park and Ang approach was mostly linear up to the ultimate limit state where the damage index reached a little higher than one. The damage index value at each ductility was almost at the same level along with increasing loading cycles, which is a disadvantage for indicating the progression of damage for different loading cycle at the same ductility. The flexural displacement ductility capacity decreased from 11 to 4.5 under T/M ratio 0.2 and 0.6, respectively. Therefore the slope of flexural damage index and displacement ductility relation curves increased along with increasing T/M ratio as shown in Figs. 14 and 15, which indicated that the progression of flexural damage is amplified with an increase in T/M ratios due to torsion effect. The torsional rotation

ductility at the ultimate state dropped from 9.5 to 6 and 2.5 when T/M ratio decreased from ∞ to 0.6 and 0.2, which also indicated the progression of torsional damage, is amplified by the flexure effect. As shown in Figs. 16 and 17, the flexural and torsional damage indices by the modified Hwang and Scribner approach increased with the progressive ductility up to ultimate value, which is much higher than the unit one by the Park and Ang approach. The damage index value of this modified model increased as more loading cycles were imposed at the each ductility, which is an advantage to demonstrate the progression of damage and stiffness degradation along with loading cycles within specific ductility. Flexural damage index by the modified Hwang and Scribner approach significantly increased with highly non-linear features after spalling of concrete cover up to ultimate damage state. Though the ultimate flexural damage indexes dropped from 11.5 to 4 for T/M ratios of 0.2 and 0.6 respectively, the column loaded with larger torsional moment (T/M=0.6) obtained larger flexural damage index at the same displacement ductility, indicating the amplification and acceleration of flexural damage limit states due to torsion effect. The torsional damage index by the modified Hwang and Scribner approach rapidly developed and became highly non-linear after yielding of the transverse spirals. The ultimate torsional damage indexes were 3.6, 3.25, and 1.35 with respect to the T/M ratios of ∞, 0.6, and 0.2 respectively. Though the ultimate torsional damage index value decreased with more flexure, the flexural effect degraded the rotation ductility capacity and amplified the torsional damage states during the progression of damage.

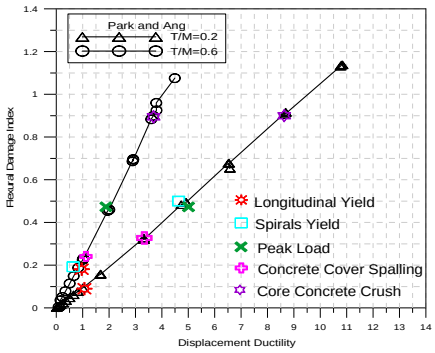

Figure 14. Park and Ang Flexural Damage Index

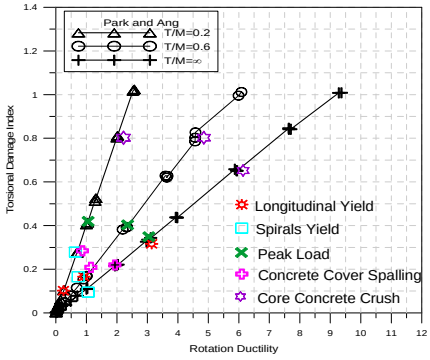

Figure 15. Modified Park And Ang Torsional Damage Index

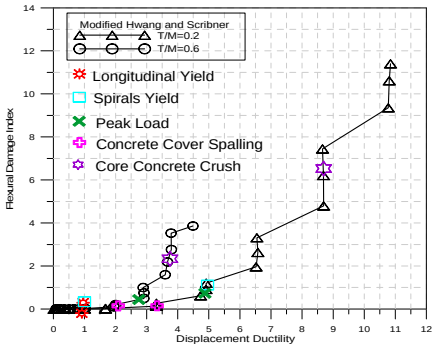

Figure 16. Modified Hwang and Scribner Flexural Damage Index

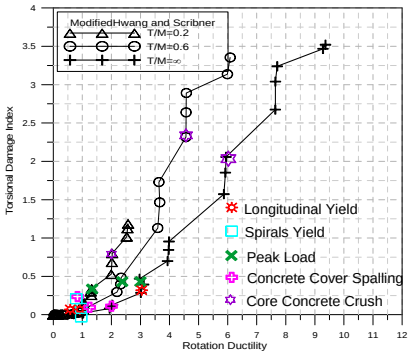

Figure 17. Modified Hwang and Scribner Torsional Damage Index

5. SUMMARY

This study evaluates the damage characteristics of RC bridge columns under combined loading including torsion by the energy dissipation and proposed damage index during various damage limit states. Decoupled damage index models for pure torsion and combined loading were proposed to study

damage progression under combined loadings according to existing damage index models. Based on the test results and discussion, the following major concluding remarks are drawn:

1) Torsional moment and rotation capacity decreased along with decreasing T/M ratios; similarly the bending moment and displacement capacity were reduced by the combination of flexure and torsion.
2) Under combined flexure and torsion, the flexural energy dissipation capacity of RC columns with interlocking spirals decreased with an increase in the T/M ratio due to the fact that torsion causes severe shear crack, more concrete cover spalling, less displacement ductility capacity, and significant stiffness degradation; and the torsional energy dissipation capacity decreased along with more flexure imposed resulting from more crushing of core concrete, buckling of longitudinal bar and less rotation ductility.
3) For the columns under flexure dominated failure mode, the dissipated torsional energy at each ductility significantly increased along with the increasing ductility up to ultimate flexure with longitudinal bar buckling/rupturing and core concrete crushing; while for the columns under torsion dominated failure mode, the dissipated torsional energy at each ductility increased along with the increasing ductility up to peak torque and then decreased for the further increase in imposed ductility due to the fact that torsional stiffness severely degraded after the concrete cover totally palled and the peak torque was achieved.
4) Though the Park and Ang damage index model was proposed to quantify the damage limit states for the flexure dominated RC columns, it could be extended to predict the progression of torsional damage for RC columns under combined loading. The damage index is physically intuitive to quantify the damage ranging from '0', indicating no damage, to '1', indicating almost collapse. But it is difficult to indicate the progression of damage for different loading cycles at the same ductility since the damage index value at each ductility was almost at the same level with respect to increasing loading cycles.
5) Normalization-modified Hwang and Scribner damage index model was proposed by normalizing the damage index with energy dissipation capacity of the columns to predict both flexural and tensional damage limit states under combined loading. The damage index value of this modified model increased as more loading cycles were imposed at each ductility, which is an advantage to demonstrate the progression of damage and stiffness degradation along with loading cycles within specific ductility.
6) According to the comparison of the flexural and torsional damage index with various T/M ratios, it is concluded that the flexural and torsional damage limit states are amplified and accelerated due to the interactive affect between flexure and torsion under the combined loading.

REFERENCE

Banon, H., Biggs, J.M. and Irvine, H.M. (1981). Seismic damage in reinforced concrete members. *Journal of Structural Engineering, ASCE* **107:9**, 1713-1729.

Hindi, R.A. and Sexsmith, R.G. (2001). A Proposed Damage Model for RC Bridge Columns under Cyclic Loading. *Earthquake Spectra* **17:2,** 261-290.

Hwang, T.H. and Scribner, C.F. (1984). R/C Member Cyclic Response during Various Loadings. *Journal of Structural Engineering, ASCE* **110:3,** 477-489.

Khashaee, P. (2005). Damage-Based Seismic Design of Structures. *Earthquake Spectra* **21:2,** 459-468.

Park, Y.J. and Ang, A.H.S. (1985). Mechanistic Seismic Damage Model for Reinforced Concrete, *Journal of Structural Engineering*, *ASCE* **111:4,** 722-739.

Roufaiel, M.S.L., and Meyer, C. (1987). Analytical modeling of hysteretic behavior of R/C frames. *Journal of Structural Engineering, ASCE* **113:3,** 429-444.

Suriya Prakash, S., and Belarbi, A. (2010).Towards Damage Based Design Approach for RC Bridge Columns under Combined Loadings Using Damage Index Models. *Journal of Earthquake Engineering* **14:3,** 363-389.

Williams, M.S., Villemure, I. and Sexsmith, R.G., "Evaluation of Seismic Damage Indices for Concrete Elements Loaded In Combined Shear And Flexure," *ACI Structural Journal* **6:1,** 37-45.

Zahrah, T.F., and Hall, W.J. (1984). Earthquake Energy Absorption in SDOF Structures. *Journal of Structural Engineering, ASCE* **110:8,** 1757-1772.